Remote Sensing of Environment 206 (2018) 254–259

Contents lists available at ScienceDirect

Remote Sensing of Environment

journal homepage: www.elsevier.com/locate/rse

The shelf-life of airborne laser scanning data for enhancing forest inventory inferences

Ronald E. McRoberts[a,*], Qi Chen[b], Dale D. Gormanson[a], Brian F. Walters[a]

[a] Northern Research Station, U.S. Forest Service, Saint Paul, MN, USA
[b] Department of Geography, University of Hawai'i at Mānoa, Honolulu, HI, USA

ARTICLE INFO

Keywords:
Model-assisted estimator
Stratified estimator
Inference

ABSTRACT

The term *shelf-life* is used to characterize the elapsed time beyond which a commodity loses its usefulness. The term is most often used with reference to foods and medicines, but herein it is used to characterize the elapsed time beyond which airborne laser scanning (ALS) data are no longer useful for enhancing inferences for forest inventory population parameters. National forest inventories (NFI) have a long history of using remotely sensed auxiliary information to enhance inferences. Although the combination of model-assisted estimators and ALS auxiliary data has been demonstrated to be particularly useful for this purpose, the expense associated with the acquisition of the ALS data has been an argument against their operational use. However, the longer the shelf-life of ALS data, the less the continuing acquisition costs and the greater the utility of the data.

The objective of the study was to assess the shelf-life of ALS data for enhancing inferences in the form of confidence intervals for mean aboveground, live tree, stem biomass per unit area. Confidence intervals were constructed using both model-assisted estimators and post-stratified estimators, four measurements of mostly the same forest inventory plots at 5-year intervals over a 17-year period, and a single set of ALS data acquired near the end of the 17-year period. The study area in north central Minnesota in the USA was characterized by naturally regenerated, uneven-aged, mixed species stands on both lowland and upland sites. The primary conclusions were twofold. First, the shelf-life of ALS data when used with model-assisted estimators exceeded 10 years, and second, even for 12 years elapsed time between plot measurement and ALS data acquisition, the variance of the model-assisted estimator of the mean was smaller by a factor of at least 1.75 than the variance of the stratified estimator used by the national forest inventory.

1. Introduction

National forest inventories (NFI) have a long history of using remotely sensed auxiliary information to enhance inferences in the form of confidence intervals for forest inventory parameters. Bickford (1952, 1960) in the United States of America (USA) and Poso (1972) in Finland used interpreted aerial photography to construct strata in support of stratified estimators. More recently, satellite imagery has been used as the source of auxiliary information for this purpose (Poso et al., 1984, 1987; McRoberts et al., 2002, 2006; Nilsson et al., 2005; Gormanson et al., 2017). For categorical forest attributes variables such as forest/non-forest, stratified estimators are effective for increasing precision, but they are less effective for continuous attributes such as aboveground biomass. For the latter attributes, airborne laser scanning (ALS) data are more effective as a source of stratification information. However, ALS data are even more effective when used with model-assisted estimators (McRoberts et al., 2013).

Although ALS data are more effective than satellite spectral data when used with both stratified and model-assisted estimators, ALS data are also expensive to acquire, whereas MODIS, Landsat and Sentinel 2 satellite spectral data are available without charge. Some countries including Austria (Hollaus et al., 2009), Sweden (Nilsson et al., 2017), and the USA (Chen et al., 2016) have acquired large area, wall-to-wall ALS data with small pulse densities for purposes of constructing digital terrain models (DTM). Although these data have been demonstrated to be useful for constructing inventory inferences, their utility is perishable in the sense that the data become less effective as the time between the date of ALS data acquisition and the date of ground plot measurements increases. Further, because DTMs are constant, multiple similar ALS acquisitions for this purpose are unlikely.

The term *shelf-life* is used to characterize the time beyond which a commodity loses its usefulness. The term is most often used with reference to foods and medicines, but it is also relevant for characterizing the utility of ALS data. Although a commodity loses usefulness because

*Corresponding author.
E-mail address: rmcroberts@fs.fed.us (R.E. McRoberts).

https://doi.org/10.1016/j.rse.2017.12.017
Received 15 June 2017; Received in revised form 8 December 2017; Accepted 14 December 2017
0034-4257/ Published by Elsevier Inc.

of change in the commodity, ALS data lose usefulness because of change in the environment in which they are used. The important point is that if ALS data can be demonstrated to have a long shelf-life, considerable cost savings may be realized by extending the time between their acquisitions.

The objective of the study was to assess the shelf-life of ALS data for enhancing inferences in the form of confidence intervals for mean aboveground, live tree, stem biomass per unit area. Confidence intervals were constructed using model-assisted estimators, four measurements of mostly the same forest inventory plots at 5-year intervals over a 17-year period, and a single set of ALS data. For a study area in north central Minnesota in the USA, average plot measurement dates for the four datasets ranged from 12 years before to three years following the date of the ALS acquisition. For assessing the shelf-life of the ALS data, model-assisted estimates of means and standard errors were compared to operational NFI estimates obtained using stratified estimators and Landsat-based strata.

2. Data

2.1. Study area

The 7583-km^2 study area consisted of the entirety of Itasca County in north central Minnesota in the USA (Fig. 1) and is characterized as approximately 80% forest land. Land cover includes water, wetlands and forest consisting of uplands with deciduous mixtures of pines, (*Pinus* spp.), spruce (*Picea* spp.), and balsam fir (*Abies balsamea* (L.) Mill.) and lowlands with spruce (*Picea* spp.), tamarack (*Larix laricina* (Du Roi) K. Koch), white cedar (*Thuja occidentalis* (L.)), and black ash (*Fraxinus nigra* Marsh.). Forest stands in the study area are typically naturally regenerated, uneven-aged, and mixed species.

2.2. Airborne laser scanning data

Wall-to-wall ALS data were acquired in April 2012 with a nominal pulse density of 0.67 pulses/m^2 using laser scanners with pulse repetition frequency of approximately 100 kHz and wavelength of 1064 nm. The Tiffs (Toolbox for Lidar Data Filtering and Forest Studies) software was used to construct a digital terrain model using all pulse returns for all heights (Chen, 2007). For both the 168.3-m^2 plots and for the 169-m^2 square cells that tessellated the study area and served as population units, distributions of pulse return heights were constructed and used to calculate ALS metrics: mean (h_{mn}), standard deviation (h_{sd}), skewness (h_{sk}), kurtosis (h_{ku}), and quadratic mean height (h_{qm}) (Lefsky et al., 1999; Chen et al., 2012). In addition, standard height and canopy density percentiles were calculated as per (Gobakken and Næsset, 2008). In particular, heights corresponding to the 10th, 20th, …, 100th percentiles (h_{10}, h_{20}, …, h_{100}) of the distributions were calculated as were canopy densities expressed as the proportions of pulse returns with heights greater than 10%, …, 90%, 95% (d_{10}, …, d_{90}, d_{95}) of the range between a minimum ALS aboveground height threshold and the 95th height percentile.

2.3. Forest inventory data

Data were obtained for plots established by the Forest Inventory and Analysis (FIA) program of the U.S. Forest Service which conducts the NFI of the USA. The FIA program has established field plot centers in permanent locations using a systematic unaligned sampling design that is regarded as producing an equal probability sample (McRoberts et al., 2010). Each FIA plot consists of four 7.32-m (24-ft) radius circular subplots that are configured as a central subplot and three peripheral subplots with centers located at 36.58 m (120 ft) and azimuths of 0°, 120°, and 240° from the center of the central subplot. Field crews observe species and measure diameter at breast-height (dbh, 1.37 m, 4.5 ft) and height for all trees with dbh of at least 12.7 cm (5 in).

Subplot-level aboveground, live tree, stem biomass was predicted for individual measured trees using allometric models, aggregated at subplot level, scaled to a per unit area basis, designated AGB, and associated with ALS metrics for the subplot. Uncertainty associated with the allometric model predictions was ignored for this study. Data were used for only the central subplots of the 359 plots measured in 2014, 2015, and 2016 because these were the only subplots and years for which plot coordinates were obtained using survey grade GPS receivers

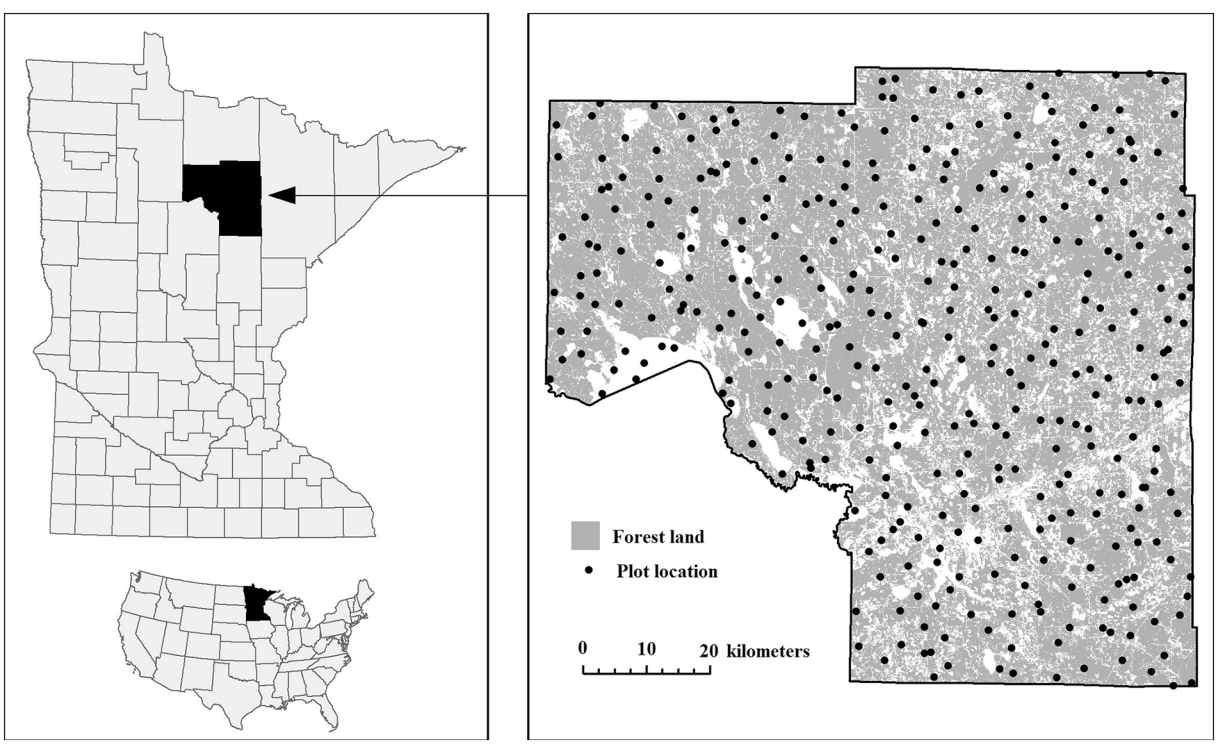

Fig. 1. Study area in Itasca County, Minnesota, USA.

with sub-meter accuracy. For future reference, the central subplots are hereafter designated *plots*.

FIA plots in the study area were measured at 5-year intervals beginning in 1999. Thus, the survey grade GPS coordinates obtained for plots measured in 2014–2016 are also applicable for the same plots measured in 1999–2001, 2004–2006, and 2009–2011. For the four 5-year measurement intervals, the 5th percentile of non-zero AGB ranged from 1.86 to 2.54 Mg/ha, the median ranged from 13.18 to 17.90 Mg/ha, and the 95th percentile ranged from 43.91 to 58.95 Mg/ha. Four datasets were constructed by combining the ALS data for the single 2012 acquisition with plot-level AGB for the four time periods.

3. Methods

3.1. Data outliers

Multiple factors affected the utility of observations for some plots. First, the FIA program classifies plots with respect to forest use, not forest cover. Therefore, plots with substantial tree-based AGB but classified as non-forest use (e.g., orchards, parkland, residential property) would not be measured in the field and would have AGB = 0 recorded. To alleviate this discrepancy, plots were deleted from further analyses if they had AGB = 0 and $h_{mn} \geq 2.0$ m. The 2.0-m threshold was selected to be slightly larger than the 1.37-m breast-height threshold for measuring trees but is acknowledged to be arbitrary. In addition, 2.0 m is often used as an ALS threshold for distinguishing between trees and ground vegetation (Gobakken and Næsset, 2008). Second, some plots classified as having forest use had AGB = 0 for one or more measurements but AGB > 0 for a subsequent measurement near the date of the ALS acquisition. These plots were likely harvested before the first measurement but had regenerated to the degree that they had measureable biomass by the date of the ALS acquisition; these plots were also deleted from further analysis. Third, some plots classified as having forest use had AGB > 0 prior to the date of the ALS acquisition but AGB = 0 subsequent to the date of ALS acquisition. To alleviate this discrepancy, plots were deleted from further analyses if they had AGB > 0 before the ALS acquisition, AGB = 0 subsequent to the ALS acquisition, and $h_{mn} \geq 2.0$ m. The latter criterion indicates the harvest was subsequent to the ALS acquisition. All deletions were considered to be observations missing at random in the sense that there was nothing unique about them relative to factors such as forest type and geographical location.

3.2. Model

An initial model of the relationship between AGB as the dependent variable and the ALS metrics as independent variables was formulated using a power model as,

$$y_i = \beta_0 \cdot x_i^{\beta_1} + \varepsilon_i, \tag{1a}$$

where i indexes plots, y_i is AGB, x_i is an ALS metric, ε_i is a random residual, and the βs are parameters to be estimated. An advantage of this model is that when the ALS metrics are zero, as is the case for typical non-forest plots, the prediction will also be zero. A forward selection procedure was used to select additional independent variables for inclusion in the exponential component of the modification of the model of Eq. (1a) expressed as,

$$y_i = \beta_0 \cdot x_{1i}^{\beta_1} \cdot \exp(\beta_2 \cdot x_{2i} + \beta_3 \cdot x_{3i} + \cdots + \beta_p \cdot x_{pi}) + \varepsilon_i, \tag{1b}$$

where p is the number of independent variables selected. The effect of the exponential component of Eq. (1b) is simply to increase or decrease the prediction based on Eq. (1a) by small increments. Additional independent variables were included if they statistically significantly increased the quality of fit of the model to the data at the $\alpha = 0.05$ level. Inclusion of additional independent variables terminated when either no additional independent variable statistically significantly increased the quality of fit of the model to the data or the increase in pseudo-R^2 (R^{2*}) was less than 0.01 where,

$$R^{2*} = \frac{SS_{mn} - SS_{res}}{SS_{res}}, \tag{2}$$

SS_{mn} is the sum of squared differences between AGB observations and their mean, and SS_{res} is the sum of squared residual deviations between AGB observations and their respective model predictions. Minor variations of this model form have been previously used successfully by Andersen et al. (2014), Chen (2015), Chen et al. (2016), and McRoberts et al. (2016).

3.3. Inference

For NFI purposes, the ultimate analytical objective is a statistical inference in the form of a confidence interval expressed as $\hat{\mu} \pm t \cdot \sqrt{V\hat{a}r(\hat{\mu})}$ where $\hat{\mu}$ is the estimator of the population mean, $V\hat{a}r(\hat{\mu})$ is the estimator of the variance of the estimator of the mean, and t corresponds to the confidence level. Thus, technical estimation for the study focused on $\hat{\mu}$ and its standard error, $SE(\hat{\mu}) = \sqrt{V\hat{a}r(\hat{\mu})}$.

3.3.1. Model-assisted estimators

Model-assisted estimators capitalize on the relationship between observations and their predictions to increase precision. A *synthetic* estimator of the population mean is,

$$\hat{\mu}_{Syn} = \frac{1}{N} \sum_{i=1}^{N} \hat{y}_i, \tag{3a}$$

where N is the population size and $\hat{y}_i$ is the model prediction of AGB for the ith population unit. Hansen et al. (1983) note that models that do not "represent the state of nature" induce bias into estimators which, for equal probability samples, can be estimated as,

$$B\hat{i}as(\hat{\mu}_{Syn}) = \frac{1}{n} \sum_{i=1}^{n} \varepsilon_i, \tag{3b}$$

where n is the sample size, and $\varepsilon_i = \hat{y}_i - y_i$. The model-assisted, *generalized regression* (GREG) estimator is then,

$$\hat{\mu}_{GREG} = \hat{\mu}_{Syn} - B\hat{i}as(\hat{\mu}_{Syn}) = \frac{1}{N} \sum_{i=1}^{N} \hat{y}_i - \frac{1}{n} \sum_{i=1}^{n} \varepsilon_i \tag{3c}$$

(Särndal et al., 1992; Särndal, 2011). The corresponding GREG variance estimator is,

$$V\hat{a}r(\hat{\mu}_{GREG}) = \frac{1}{n(n-p)} \sum_{i=1}^{n} (\varepsilon_i - \bar{\varepsilon})^2, \tag{3d}$$

where p is the number of model parameters and $\bar{\varepsilon} = \frac{1}{n} \sum_{i=1}^{n} \varepsilon_i$ (Särndal et al., 1992; Särndal, 2011).

3.3.2. Stratified estimators

Because the FIA program uses post-stratified estimators for the study area, estimates based on these estimators were also calculated for comparison purposes. The FIA program's post-stratified estimators are based on five strata derived from the 2011 National Land Cover Dataset tree canopy cover dataset which includes percent tree canopy cover values in the range of 0%–100% percent for 30-m × 30-m pixels (Huang et al., 2001). For the study area, FIA strata consist of pixels within specified percentage tree canopy cover ranges: 0–5%, 6–50%, 51–65%, 66–80% and 81–100% (Gormanson et al., 2017). Estimates of population means are calculated using the unbiased stratified estimator,

$$\hat{\mu}_{Str} = \sum_{h=1}^{H} w_h \hat{\mu}_h, \tag{4a}$$

where

$$\hat{\mu}_h = \frac{1}{n_h} \sum_{i=1}^{n_h} y_{hi},$$

h = 1, …H denotes strata; y_{hi} is the ith sample observation for the hth stratum; w_h is the weight for the hth stratum calculated as the proportion of population units assigned to the stratum; n_h is the number of plots assigned to the hth stratum; $\hat{\mu}_h$ and $\hat{\sigma}_h^2$ are the sample estimates of the within-stratum mean and variance, respectively (Cochran, 1977).

Because the FIA program uses permanent plots and a spatially constant sampling intensity, stratifications are constructed independently of the sampling, a technique characterized as post-sampling stratification or simply *post-stratification*. Cochran (1977, p. 135) provides a post-stratified estimator of the variance that accommodates the random within-strata sample sizes,

$$\hat{Var}(\hat{\mu}_{Str}) = \sum_{h=1}^{H} w_h \frac{n_h}{n} \frac{\hat{\sigma}_h^2}{n_h} + \frac{1}{n} \sum_{h=1}^{H} (1\text{-}w_h) \frac{n_h}{n} \frac{\hat{\sigma}_h^2}{n_h}, \tag{4b}$$

where

$$\hat{\sigma}_h^2 = \frac{1}{n_h\text{-}1} \sum_{i=1}^{n_h} (y_{hi}\text{-}\hat{\mu}_h)^2,$$

and n is the total sample size over all strata.

Because the basis for deleting outliers (Section 3.1) is related to differences between the dates of plot measurements and the ALS acquisition date, and because the post-stratified estimators do not use the ALS data, no outliers were deleted when applying these estimators.

4. Results and discussion

4.1. Outliers

Three categories of plots were deleted from the analyses. First, 50 plots with trees but classified as non-forest by FIA field crews were deleted from the analyses; however, these deletions represented only 29 different plots, because some plots were deleted for multiple datasets. For these deleted plots, mean ALS heights ranged from 2.07 to 9.34 m and 95th percentiles of ALS heights ranged from 6.11 to 25.02 m, both of which indicate measurable trees on the plots. Second, 25 forest plots with AGB = 0 but with ALS heights consistent with AGB > 0 were deleted; these deletions represented only 20 different plots, because some plots were deleted for multiple datasets. At the time of their measurements, these plots had AGB = 0, but by the later ALS acquisition date had measurable trees and AGB > 0 as indicated by their 95th percentiles of ALS heights which ranged from 4.21 to 20.52 m. Third, seven forest plots with AGB > 0 at the ALS acquisition date but AGB = 0 at the plot measurement date were deleted; these were all different plots. For these deleted plots, the 95th percentiles of ALS heights ranged from 10.68 to 24.88 m, clearly indicating the presence of measurable trees at the ALS acquisition date. For the four datasets, the proportions of plots deleted ranged from 0.04 to 0.09 with greater proportions for datasets whose plot measurement dates deviated more from the ALS acquisition date.

4.2. Models

The fits of the models to the data produced R^{2*} ranging from 0.61 for the 1999–2001 dataset to 0.77 for the 2014–2016 dataset (Table 1) (Fig. 2). These R^{2*} values are similar to those reported by Næsset et al. (2011) and McRoberts et al. (2013) for two Norwegian study areas, by Strunk et al. (2012) for a study area in Washington, USA, and by d'Oliveira et al. (2012) for a Brazilian study area. The final forms of the models as represented by Eq. (1b) included either three or four independent variables. For the initial, power form of the model as represented by Eq. (1a), h_{qm} was always the independent variable selected. R^{2*} for this power form of the model ranged from 0.47 for the 1999–2001 dataset to 0.68 for the 2014–2016 dataset; these R^{2*} values represented 66–97% of the R^{2*} values obtained for the final model form represented by Eq. (1b). The additional selected independent variables varied considerably but were generally lower and middle height and density metrics. Finally, deletion of some plots as described in Sections 3.1 and 4.1 did not increase R^{2*} by more than 0.11.

4.3. Inference

For the GREG estimators, two sets of bias estimates as per Eq. (3b) were calculated, one set for the datasets used to fit the models and a second set that also included the non-forest plots with trees. Subtraction of the first set of bias estimates produced AGB estimates for all lands, whereas subtraction of the second set of bias estimates produced AGB estimates consistent with the FIA program's definition of forest land: (i) minimum area 0.4 ha (1.0 ac), (ii) minimum tree cover of 10%, (iii) minimum width of 36.58 m (120 ft), and (iv) forest land use. As expected, estimates for all lands were larger than estimates for forest land (Table 1). The differences in the estimates, with mean 2.58 Mg/ha and ranging from 1.32 to 4.22 Mg/ha, can be interpreted as mean biomass on non-forest land with trees. The GREG estimates of AGB for forest land were slightly larger than the FIA estimates but were not statistically significantly different (Table 1).

The GREG standard errors for all lands were slightly smaller than the GREG standard errors for forest land. This result is as expected because the model predicts positive AGB for non-forest land with trees, whereas the FIA program assigns AGB = 0 for these lands. When calculating variances using Eq. (3d), the larger residuals for the plots on non-forest lands with trees are included for forest land but not for all lands.

For forest land, the GREG standard errors were substantially smaller than the stratified standard errors by 26.6% for 1999–2001 to 41.0% for 2014–2016. As expected, standard errors increased as elapsed time between the plot measurement dates and the ALS acquisition date increased. Of importance, sample sizes to achieve selected precision criteria are proportional to variances calculated as squares of standard errors, not to the standard errors themselves. Thus, the ratios of variances which ranged from 1.79 to 2.87 represent the factors by which sample sizes for the stratified estimators would have to have been increased to achieve the same standard errors as were achieved using the GREG estimators. Alternatively, the latter ratios represent the factors by which sample sizes could be reduced with no loss of precision when using the GREG estimators rather than the stratified estimators.

4.4. Consequences

The most important consequence is that for NFIs such as the FIA program, model-assisted estimators with ALS auxiliary data have the potential to reduce sampling costs with no loss of precision. For plot measurement dates within 2–3 years of the ALS acquisition date, GREG variances were smaller than stratified variances by factors greater than 2.5, and for plots measured 7–12 years before the ALS acquisition date, smaller by factors greater than 1.75. Further, the relative diversity of the naturally regenerated, uneven-aged, mixed species forests with more than 25 observed species on both lowland and upland sites suggests that the results may be generally applicable for temperate forests.

Several caveats must be observed, however. First, the ALS data must be available. If not, then the cost of ALS acquisition could be offset by reductions in sampling intensities. Although the natural inclination would be to synchronize ALS acquisitions with the FIA program's 5-year cycle, the results of this study suggest that elapsed time between acquisitions could be extended to as many as 10 years. For purposes of

Table 1
Estimates of aboveground, live tree, stem biomass.

Years	Generalized regression estimators							FIA stratified estimators		
	R^{2*}	All land[a]			Forest land[b]			Forest land		
		n	$\hat{\mu}_{GREG}$	$SE(\hat{\mu}_{GREG})$	n	$\hat{\mu}_{GREG}$	$SE(\hat{\mu}_{GREG})$	n	$\hat{\mu}_{Str}$	$SE(\hat{\mu}_{Str})$
1999–2001	0.61	238	39.90	1.99	247	35.68	2.10	257	31.74	2.86
2004–2006	0.63	278	33.87	1.76	294	31.09	1.86	307	29.52	2.49
2009–2011	0.70	344	35.12	1.54	356	33.80	1.57	358	31.92	2.52
2014–2016	0.77	302	36.24	1.56	315	34.24	1.64	322	34.19	2.78

[a] Excludes plots with trees on non-forest land (Section 4.3).
[b] Includes plot with trees on non-forest land (Section 4.3).

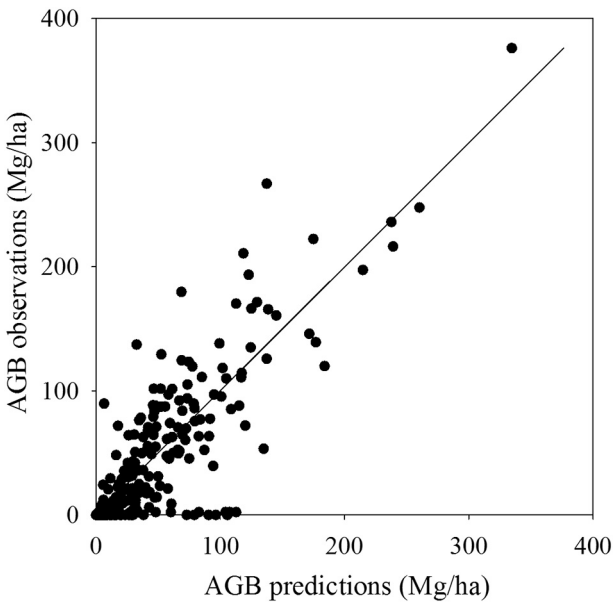

Fig. 2. Observed versus predicted AGB for the 2014–2016 dataset.

stratification, the FIA program currently uses a tree canopy cover product that is only updated approximately every 10 years (Homer et al., 2015), so there is a precedent for 10-year intervals between acquisitions of auxiliary data. Second, if sampling intensities are reduced to offset ALS acquisition costs, sufficient sample sizes must remain to construct the models. As elapsed time between ALS acquisitions and plot measurements increases, more plots will need to be deleted as outliers as a result of more harvesting, deforestation, and regeneration. Although deletions were less than 10% for this study, percentages will differ depending on factors such as harvest rates, forest composition, fragmentation, and the distribution of land uses. Third, from an operational perspective, plot measurements would typically follow rather than precede the ALS acquisition as is the case for some datasets for this study. Although similar results would be expected, the issue should be investigated in greater detail.

Finally, interest is increasing in attributes of non-forest land with trees, also characterized internationally as *trees outside forests* (TOF, de Foresta et al., 2013). For example, Meneguzzo et al. (2013) note that TOF protect soil and water resources, provide wildlife habitat, contribute to farmstead energy efficiency and aesthetics, and sequester carbon. Johnson et al. (2014) reported that in Maryland in the mid-Atlantic region of the USA, 21–27% of predicted live tree biomass was on land the FIA program classifies as non-forest. For agricultural states in the Midwestern region of the USA, Perry et al. (2009) estimate the area of all tree-covered lands exceeds the area of forest land by 25–38%. Thus, methods such as developed for this study that can produce estimates for all land, not just forest land, but use only plot observations for forest land, merit consideration.

5. Conclusions

Two primary conclusions were drawn from the study. First, in the context of inventory inferences, the shelf-life of airborne laser scanning data when used with model-assisted estimators was at least 10 years. If so, the cost of acquiring these auxiliary data, often regarded as limiting factor for their operational use, can be substantially reduced. Second, even for 12 years elapsed time between plot measurement and airborne laser scanning data acquisition, the model-assisted estimators reduced the variance of the estimator of mean aboveground, live tree, stem biomass by 75% relative to variances obtained using stratified estimators.

Three options for offsetting the costs of airborne laser scanning data acquisition by reducing sampling can be considered: (i) reduce the number of plots measured each year, (ii) reduce the number of subplots measured for each plot, and (iii) use a single slightly larger plot at each sampling location. As previously, sampling intensity reductions by factors of 1.75–2.50 would not adversely affect precision. Because of the large correlations among observations for subplots of the same FIA plot, reduction of the aggregated area of FIA's four subplots by a factor of 2.0 via either the second or third option would reduce precision by a factor considerably < 2.0. Further, if a single plot with twice the area of a current FIA subplot were used at each sampling location, the resulting 335-m^2 FIA plot would still be smaller than the much more commonly used 500-m^2 NFI basic sampling unit (Tomppo et al., 2010, NFI Reports). Further, the larger plot size would be more amenable for use with remotely sensed auxiliary data (Vauhkonen et al., 2014, p. 6).

References

Andersen, H.-E., Reutebuch, S.E., McGaughey, R.J., d'Oliveira, M.V.N., Keller, M., 2014. Monitoring selective logging in western Amazonia with repeat lidar flights. Remote Sens. Environ. 151, 157–165.
Bickford, C.A., 1952. The sampling design used in the forest survey of the northeast. J. For. 50, 290–293.
Bickford, C.A., 1960. A test of continuous inventory for National Forest management based upon aerial photographs, double sampling, and remeasured plots. In: Anonymous (Ed.), Proceedings of the Society of American Foresters Meeting, November 15-19, 1959, San Francisco, California. Society of American Foresters, Washington, DC, pp. 143–148.
Chen, Q., 2007. Airborne lidar data processing and information extraction. Photogramm. Eng. Remote. Sens. 73 (12), 1355–1365.
Chen, Q., 2015. Modeling aboveground tree woody biomass using national-scale allometric methods and airborne lidar. ISPRS J. Photogramm. Remote Sens. 106, 95–106.
Chen, Q., Vaglio Laurin, G., Battles, J.J., Saah, D., 2012. Integration of airborne lidar and vegetation types derived from aerial photography for mapping aboveground live biomass. Remote Sens. Environ. 121, 108–117.
Chen, Q., McRoberts, R.E., Wang, C., Radtke, P.J., 2016. Forest aboveground biomass mapping and estimation across multiple spatial scales using model-based inference. Remote Sens. Environ. 184, 350–360.
Cochran, W.G., 1977. Sampling techniques, 3rd edition. Wiley, New York.
d'Oliveira, M.V.N., Reutebuch, S.E., McGaughey, R.J., Andersen, H.-E., 2012. Estimating Forest biomass and identifying low-intensity logging areas using airborne scanning lidar in Antimary State Forest, Acre State, Western Brazilian Amazon. Remote Sens. Environ. 124, 479–491.

de Foresta, H., Somarriba, E., Temu, A., Boulanger, D., Feuilly, H., Gauthier, M., 2013. Towards the assessment of trees outside forests. In: Resources Assessment Working Paper. 183 Rome, FAO.

Gobakken, T., Næsset, E., 2008. Assessing effects of laser point density, ground sampling intensity, and field plot sample size on biophysical stand properties derived from airborne laser scanner data. Can. J. For. Res. 38, 1095–1109.

Gormanson, D.D., Pugh, S.A., Barnett, C.J., Miles, P.D., Morin, R.S., Sowers, P.A., Westfall, J., 2017. Statistics and quality assurance for the Northern Research Station Forest Inventory and Analysis Program, 2016. In: General Technical Report NRS-166. U.S. Department of Agriculture, Forest Service, Northern Research Station, Newtown Square, PA 23 p. https://www.nrs.fs.fed.us/pubs/53730, Accessed date: April 2017.

Hansen, M.H., Madow, W.G., Tepping, B.J., 1983. An evaluation of model dependent and probability-sampling inferences in sample surveys. J. Am. Stat. Assoc. 78, 776–793.

Hollaus, M., Dorigo, W., Wagner, W., Schadauer, K., Höfle, B., Maier, B., 2009. Operational wide-area stem volume estimation based on airborne laser scanning and national forest inventory data. Int. J. Remote Sens. 30 (19), 5159–5175.

Homer, C.G., Dewitz, J.A., Yang, L., Jin, S., Danielson, P., Xian, G., Coulston, J., Herold, N.D., Wickham, J.D., Megown, K., 2015. Completion of the 2011 National Land Cover Database for the conterminous United States: representing a decade of land cover change information. Photogramm. Eng. Remote. Sens. 81 (5), 345–354.

Huang, C., Yang, Limin, Wylie, B.K., Homer, C., 2001. A strategy for estimating tree canopy density using Landsat 7 ETM + and high resolution images over large areas. In: Proceedings of the Third International Conference on Geospatial Information in Agriculture and Forestry, Denver, Colorado, 5–7 November, 2001, Available at: http://digitalcommons.unl.edu/usgspubs/111/, Accessed date: July 2017.

Johnson, K.D., Birdsey, R., Finley, A.O., Swantaran, A., Dubayah, R., Wayson, C., 2014. Integrating forest inventory and analysis data into a LIDAR-based carbon monitoring system. Carbon Balance Manag. 9, 3.

Lefsky, M.A., Harding, D., Cohen, W.B., Parker, G., Shugart, H.H., 1999. Surface lidar remote sensing of basal area and biomass in deciduous forests of eastern Maryland, USA. Remote Sens. Environ. 67, 83–98.

McRoberts, R.E., Wendt, D.G., Nelson, M.D., Hansen, M.D., 2002. Using a land cover classification based on satellite imagery to improve the precision of forest inventory area estimates. Remote Sens. Environ. 81, 36–44.

McRoberts, R.E., Holden, G.R., Nelson, M.D., Liknes, G.C., Gormanson, D.D., 2006. Using satellite imagery as ancillary data for increasing the precision of estimates for the Forest inventory and analysis program of the USDA Forest Service. Can. J. For. Res. 36, 2968–2980.

McRoberts, R.E., Hansen, M.H., Smith, W.B., 2010. United States of America. In: Tomppo, E., Gschwantner, T., Lawrence, M., McRoberts, R.E. (Eds.), National Forest Inventories, Pathways for Common Reporting. Springer 610 p.

McRoberts, R.E., Næsset, E., Gobakken, T., 2013. Inference for lidar-assisted estimation of forest growing stock volume. Remote Sens. Environ. 128, 268–275.

McRoberts, R.E., Chen, Q., Domke, G.M., Ståhl, G., Saarela, S., Westfall, J.A., 2016. Hybrid estimators for mean aboveground carbon per unit area. For. Ecol. Manag. 378, 44–56.

Meneguzzo, D.M., Liknes, G.C., Nelson, M.D., 2013. Mapping trees outside forests using high-resolution aerial imagery: a comparison of pixel- and object-based classification approaches. Environ. Monit. Assess. 185, 6261–6275.

Næsset, E., Gobakken, T., Solberg, S., Gregoire, T.G., Nelson, R., Ståhl, G., Weydahl, D., 2011. Model-assisted regional forest biomass estimation using LiDAR and InSAR as auxiliary data: a case study from a boreal forest area. Remote Sens. Environ. 115, 3599–3614.

Nilsson, M., Holm, S., Reese, H., Wallerman, J., Engberg, J., 2005. Improved forest statistics from the Swedish National Forest Inventory by combining field data and optical satellite data using post-stratification. In: Olsson, H. (Ed.), Proceedings of ForestSat 2005, Bora°s, Sweden, May 31_June, 3 2005. Jönköping: National Board of Forestry, Sweden, pp. 22–26.

Nilsson, M., Nordkvist, K., Jonzén, J., Lindgren, N., Axensten, P., Wallerman, J., Egberth, M., Larsson, S., Nilsson, L., Olsson, H., 2017. A nationwide forest attribute map of Sweden predicted using airborne laser scanning data and field data from the National Forest Inventory. Remote Sens. Environ. 194, 447–454.

Perry, C.H., Woodall, C.W., Liknes, G.C., Schoeneberger, M.M., 2009. Filling the gap: improving estimates of working tree resources in agricultural landscapes. Agrofor. Syst. 75, 91–101.

Poso, S., 1972. A Method for Combining Photo and Field Samples in Forest Inventory. 76. Communicationes Instituti Forestalis Fenniae, pp. 1–133.

Poso, S., Hame, T., Paananen, R., 1984. A method of estimating the stand characteristics of a forest component using satellite imagery. Silva Fennica 18, 261–292.

Poso, S., Paananen, R., Simila, M., 1987. Forest inventory by compartments using satellite imagery. Silva Fennica 21, 69–94.

Särndal, C.-E., 2011. Combined inference in survey sampling. Pak. J. Stat. Oper. Res. 27 (4), 359–370.

Särndal, C.-E., Swensson, B., Wretman, J., 1992. Model Assisted Survey Sampling. Springer, New York.

Strunk, J.L., Reutebuch, S.E., Andersen, H.-E., Gould, P.J., McGaughey, R.J., 2012. Model-assisted forest yield estimation with light detection and ranging. West. J. Appl. For. 27 (2), 53–59.

Tomppo, E., Gschwantner, T., Lawrence, M., McRoberts, R.E., 2010. National Forest Inventories: Pathways for Common Reporting. Springer, Dordrecht.

Vauhkonen, J., Maltamo, M., McRoberts, R.E., Næsset, E., 2014. In: Maltamo, M., Næsset, E., Vauhkonen, J. (Eds.), Forestry Applications of Airborne Laser Scanning: Concept and Case Studies. Springer, Dordrecht.